



Contents lists available at ScienceDirect

Bioorganic & Medicinal Chemistry

journal homepage: www.elsevier.com/locate/bmc

Total synthesis and antileukemic evaluations of the phenazine 5,10-dioxide natural products iodinin, myxin and their derivatives

Elvar Örn Viktorsson^a, Bendik Melling Grøthe^b, Reidun Aesoy^c, Misbah Sabir^c, Simen Snellingen^b, Anthony Prandina^a, Ove Alexander Høgmoen Åstrand^a, Tore Bonge-Hansen^b, Stein Ove Døskeland^d, Lars Herfindal^c, Pål Rongved^{a,*}

^a Department of Pharmaceutical Chemistry, School of Pharmacy, University of Oslo, PO Box 1068 Blindern, N0316 Oslo, Norway

^b Department of Chemistry, University of Oslo, PO Box 1033, Blindern, 0315 Oslo, Norway

^c Centre for Pharmacy, Department of Clinical Science, University of Bergen, Jonas Lies vei 87, N-5009 Bergen, Norway

^d Department of Biomedicine, University of Bergen, Jonas Lies vei 91, N-5009 Bergen, Norway

ARTICLE INFO

Article history:

Received 4 January 2017

Revised 22 February 2017

Accepted 25 February 2017

Available online xxxxx

Keywords:

Phenazines

Phenazine 5,10-dioxides

Acute myeloid leukemia

Hypoxia selectivity

ABSTRACT

A new efficient total synthesis of the phenazine 5,10-dioxide natural products iodinin and myxin and new compounds derived from them was achieved in few steps, a key-step being 1,6-dihydroxyphenazine di-*N*-oxidation. Analogues prepared from iodinin, including myxin and 2-ethoxy-2-oxoethoxy derivatives, had fully retained cytotoxic effect against human cancer cells (MOLM-13 leukemia) at atmospheric and low oxygen level. Moreover, iodinin was for the first time shown to be hypoxia selective. The structure-activity relationship for leukemia cell death induction revealed that the level of *N*-oxide functionality was essential for cytotoxicity. It also revealed that only one of the two phenolic functions is required for activity, allowing the other one to be modified without loss of potency.

© 2017 Published by Elsevier Ltd.

1. Introduction

Phenazines (PHZ's, Fig. 1) are *N*-heterocyclic aromatic compounds found widely in terrestrial and aquatic environments. Genera of *Pseudomonas* and *Streptomyces* are among the richest natural sources, although most of the >6000 PHZ's described are of synthetic origin.^{1–3} Hundreds of PHZ structures display biological activities, such as antitumor-,^{4–6} anti-infective-,^{7,8} anti-inflammatory,⁹ and immune-suppressive effects.¹⁰ *Pseudomonas aeruginosa*'s pyocyanin induces neutrophil death via mitochondrial reactive oxygen species and mitochondrial acid sphingomyelinase.¹¹ Various modes of action have been assigned for their biological effects, like DNA-intercalation,⁶ inhibition of topoisomerases,¹ metal chelation¹² and production of reactive oxygen species (ROS).¹³ The latter is most prominent for the subclass of PHZ 5,10-dioxides. Some of these oxides can be bio-reduced to form free hydroxyl radicals, and more so under hypoxic conditions.^{13–15} These features render the PHZ 5,10-dioxides particularly valuable as starting points for drug discovery, aimed to identify potential antitumor agents which selectively promote apoptotic cell death at low levels of oxygen saturation.

Iodinin (**2**) and myxin (**3**) (Fig. 1) are well-known natural products.⁴ Iodinin was first identified by Davis in 1939 within bacterial cultures of *Chromobacterium iodinum*¹⁶ (later re-classified as *Brevibacterium iodinum*), and its antimicrobial features described shortly after by McIlwain.^{4,17,18} Since then, various genera of bacteria producing the deep purple pigment have been identified.^{1,4} Recently, iodinin (**2**) was isolated from marine actinomycetes bacterium collected from sediment samples in the Trondheim fjord of Norway.^{19,20} Screens showed iodinin (**2**) to possess cytotoxic features with high selectivity towards acute myeloid leukemia (AML) and acute promyelocytic leukemia (APL) cells (EC₅₀ values for apoptotic cell death up to 40 times lower than for various normal cells). Remarkably, iodinin (**2**) promoted apoptotic cell death in cell-lines characterized by genetic features of poor patient prognosis.^{5,20} Myxin (**3**) displays an unusually attractive antimicrobial profile for a PHZ; potent broad spectrum activity against both Gram positive and -negative bacteria and fungi.⁷

Earlier findings indicate iodinin (**2**) and myxin (**3**) to have ability to interact with DNA through intercalation, especially with the C-G base pair of DNA, as documented for myxin (**3**),⁶ which can inhibit DNA template controlled RNA synthesis.²¹ Moreover, myxin (**3**) has recently been shown to cause radical mediated DNA strand cleavage and to promote cytotoxic events in the human colorectal cancer cell line HCT-116 under aerobic and anaerobic conditions.¹³

* Corresponding author.

E-mail address: pal.rongved@farmasi.uio.no (P. Rongved).

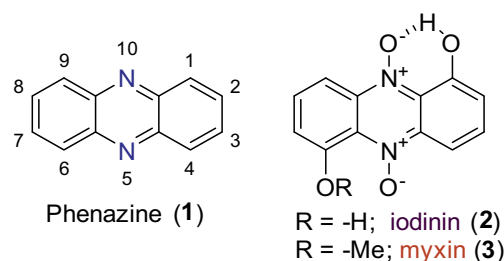


Fig. 1. The phenazine core (1) with numbered positions and the phenazine 5,10-dioxide natural products iodinin (2) and myxin (3).

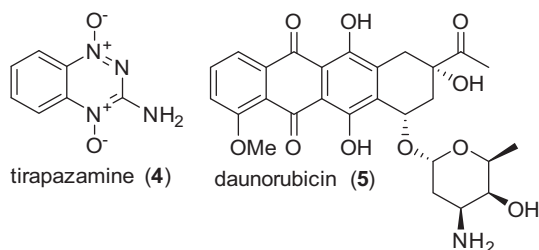


Fig. 2. The structure of tirapazamine, a hypoxia selective cytotoxic prodrug and daunorubicin, a DNA-intercalator used for the treatment of acute myeloid leukemia.

The mode of action is reported to be the same or similar as for tirapazamine (4) (Fig. 2),¹³ one of the most documented hypoxia-selective cytotoxic agents known. Tirapazamine (4) has been subjected to phase I, II and III clinical trials to treat various forms of cancer, and clinical efficacy reported in some cases, especially in combination with cis-platin.²² Chowdhury et al. showed that Phenazine 5,10-dioxides may undergo reduction of a single electron intracellularly.¹³ These events afford oxygen sensitive radicals of the heterocyclic aromatic *N*-oxide. Thus under normoxic conditions, the radicalized derivative is immediately converted back to the mother compound. In hypoxic environment however, life span of such drug-radical is prolonged and can lead to the formation of highly cytotoxic species through loss of one *N*-oxide from the scaffold.^{13,23}

Exploiting the advantage of tumor hypoxia in cancer therapy is an active research field, in part due to the fact that areas of tumor tissue can be very oxygen deficient as the result of rapid cell

growth and incomplete vascularization.²⁴ In addition, cancer cells within hypoxic regions are often resistant to chemotherapy due to upregulation of hypoxia-induced survival gene products.²⁵ However, this challenge can also provide a window of opportunity for pro-drugs activated selectively in oxygen deficit tumor tissues.²⁶

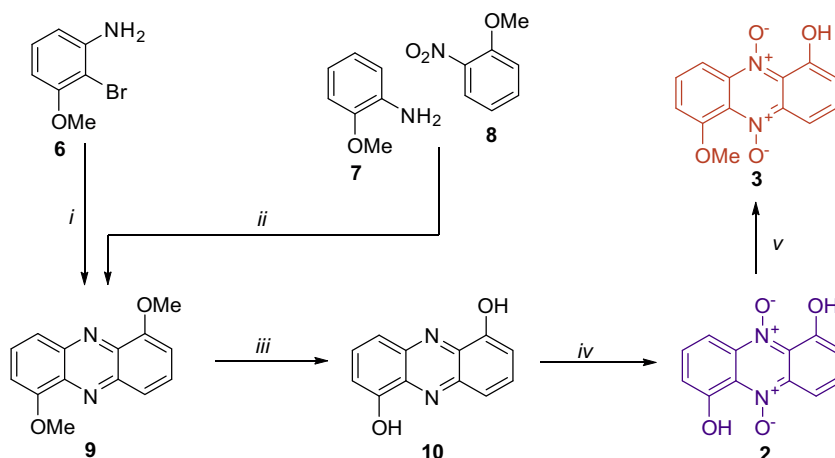
AML is the most common malignant myeloid cancer in adults, and its yearly prevalence increases to near 18 cases per 100,000 at high age.²⁷ Advances in treatments like allogeneic stem cell transplantation have mostly benefited younger patients, and the preferred chemotherapy today was developed more than 40 years ago.^{28,29} Current standards in clinic, such as daunorubicin (5) (Fig. 2), are unselective and have toxic-, sometimes lethal, side effects.^{4,28} Thus, new therapeutic agents which target leukemia more selectively are called for. On forehand, iodinin (2) has an attractive profile as lead candidate in the quest of finding new and more selective therapies against AML.⁵ However, the compound is not readily available and is known to be notoriously insoluble in aqueous and organic media.⁷

Our primary goal in the present work was to develop an iodinin-based new potential drug candidate for AML therapy. To achieve this, it was mandatory to develop a new effective synthetic route towards iodinin (2) from readily available chemical sources. In the synthetic process, the crucial step would be the oxidation forming both *N*-oxides simultaneously on the 1,6-di-*O*-substituted PHZ scaffold. Judged by synthetic procedures in prior literature,^{13,30} this step was anticipated to be the most challenging to achieve efficiently. Due to structural resemblance, myxin (3) would also be prepared from iodinin (2) as myxin's (3) antileukemic effects were unknown by forehand. A second goal was to explore the *N*-oxide role of importance in terms of cytotoxicity and further, if the phenols of iodinin (2) could be derivatized by alkylation without compromising the biological activity on leukemic cell death.

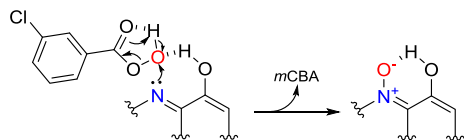
2. Results and discussion

2.1. Synthesis

The first phase of development of a synthetic route was aimed to provide 1,6-dimethoxyphenazine (9) from readily available commercial sources. To achieve this, two different approaches were explored, both of which avoid formation of PHZ regioisomers (Scheme 1). On one hand, a Pd-catalyzed double Buchwald-Hartwig C-N cross-coupling of 2-bromo-3-methoxyaniline (6)



Scheme 1. Synthesis outline and reaction conditions: i) Pd(II)-Brettphos, KHMDs (cat.) Cs₂CO₃, PhMe, reflux 24 h, 79%. ii) KOH, PhMe, 80 °C, 6%, iii) BBr₃, reflux, 5 h, >99% iv) mCPBA, PhMe, 80 °C, 6 h, 76%. v) MeI, K₂CO₃, 18-Crown-6, DMF, rt, 24 h, 61–72%.



Scheme 2. A plausible mechanism of action for the *m*CPBA oxidation where the phenol hydrogen atoms of 1,6-dihydroxyphenazine (**10**) have a coordinating effect as the per-acid approaches which results in the formation of an N-O bond.

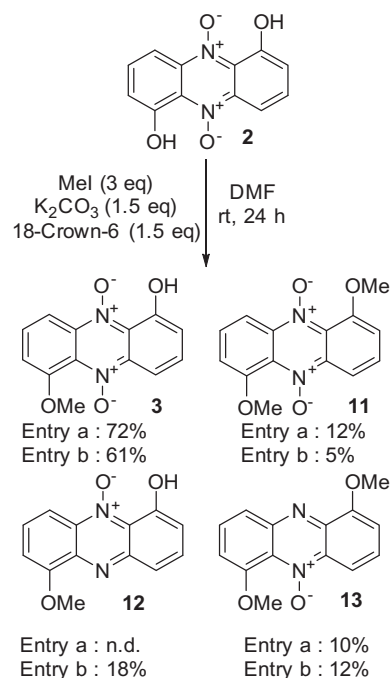
was performed, based on the reported work of Winkler et al.³¹, yielding the self-condensed product in 79% yield on a one gram scale (scheme 1). After screening of various Pd-catalysts (Table S-1 in Supplementary information), the best results were obtained using the commercially available Pd(II)-Brettphos precatalyst. Activating bases (Et₃N, KOrBu, LiHMDS and KHMDS) in combination with the precatalyst were screened, and KHMDS was found to keep the catalyst active for the longest time, also providing instant activation upon complete base addition. On the other hand, a Wohl-Aue reaction^{32,33} was undertaken condensing *o*-anisidine (**7**) and 2-nitroanisole (**8**) under strong alkaline conditions in toluene. Isolated yields from the crude black tar disappointingly afforded 6% yield of **9**. Although low yields were as expected from literature,^{13,33} one can argue that gram quantities were acquired from inexpensive starting materials using this method.

In the 2nd step of the synthesis, **9** was subjected to demethylating conditions refluxing in neat BBr₃,³⁴ which afforded 1,6-dihydroxyphenazine (**10**) quantitatively and reproducibly.

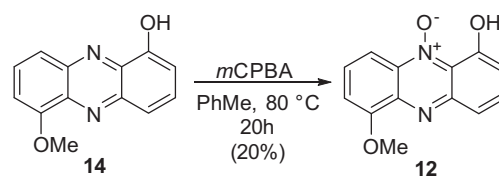
As the route to **10** was established, the synthesis of iodinin (**2**) was solely depending on the di-*N*-oxidation of the PHz scaffold. Early studies conducted by Yosioka and Kidani,³⁰ afforded iodinin (**2**) in 21% yield where 30% H₂O₂ in the presence of acetic anhydride was employed. This procedure did not prove to be reproducible in our hands. Several oxidizing reagents were tested where only *m*CPBA proved to be efficient (Table S-2 Supplementary information provides an overview over 30 entries). *m*CPBA in dichloroethane at 80 °C afforded 21% yield of iodinin (**2**) while yields were dramatically increased with toluene as solvent, which resulted in 76% yield of isolated material. In order to achieve this, *m*CPBA was added portion-wise every hour during the 6 h reaction time span. A proposed mechanism for the reaction is depicted in Scheme 2. Purification of iodinin (**2**) was easily achieved using filtration and washing with a series of solvents, which do not dissolve iodinin (**2**) like aqueous NaHCO₃, MeOH and Et₂O. The robustness of the reaction is demonstrated by the fact that it is efficient on more than 1 g scale. As many PHz 5,10-dioxides are biologically active and of growing interest, especially in terms of cancer and antibacterial research, we believe this oxidation approach might pave the way for higher synthetic versatility of compounds within literature containing the PHz 5,10-dioxide scaffold.

Methylating conditions were explored in order to synthesize myxin (**3**) from iodinin (**2**). The transformation was executed using a combination of MeI, K₂CO₃, and 18-Crown-6-ether in DMF which previously has been used to mono-*O*-methylate structurally related phenazine 5,10-dioxides.¹⁵ This method avoids using Me₂SO₄ and KOrBu in hexamethylphosphoric triamide (HMPT) which was used by Weigle's et al. to convert iodinin (**2**) cultured in bacteria to myxin (**3**).^{7,35}

The highest yields of myxin (**3**) were obtained where iodinin (**2**) was exposed to 3 eq. of MeI in presence of 1.5 eq. of K₂CO₃/18-crown-6 in DMF (room temperature, 24 h). This method gave 62–72% yield of isolated myxin (**3**) (see entries a and b, Scheme 3). However, yields proved difficult to reproduce as the solubility of myxin (**3**) is greater than of iodinin (**2**) and formation of di-*O*-methylated- (**11**) and deoxygenated by-products **12** and **13** are unavoidable. These compounds were isolated as well and tested for biological activity.



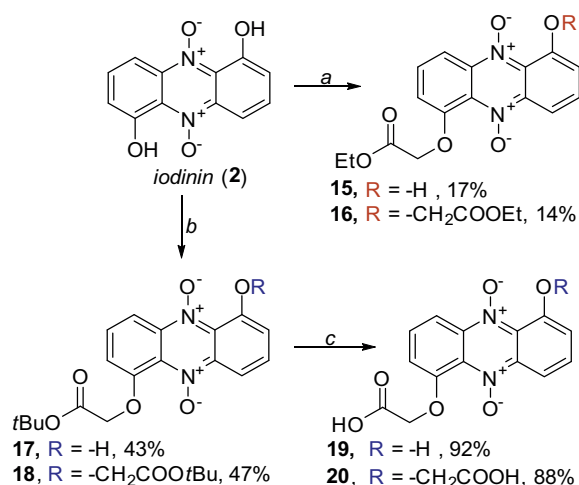
Scheme 3. Isolated compounds from two identical entries marked entry a and entry b. Compounds **11**, **12** and **13** were isolated as byproducts resulting from dialkylation, deoxygenation or both as in **13**. Table S-3 (Supplementary information) lists reaction conditions for more entries achieving this transformation.



Scheme 4. An alternative route towards myxin (**2**) was explored. Upon *m*CPBA oxidation of **14**, only formation of the mono-oxide **12** was detected by TLC analysis. This route was therefore abandoned.

An alternative route to myxin (**3**) was explored in our attempt to oxidize the myxin-scaffold 1-hydroxy-6-methoxyphenazine (**14**) (Scheme 4). However, *m*CPBA oxidation of **14** under the same conditions as used for the oxidation of 1,6-dihydroxyphenazine (**10**) to give iodinin (**2**), afforded only the mono-oxidized product 1-hydroxy-6-methoxyphenazine 10-oxide (**12**). We propose two main reasons for this phenomenon. First, the methoxy group in the 6th position does not support the peracid mechanism as depicted in Scheme 2 in the case of **10**. Secondly, myxin (**3**) turned out to be unstable at temperatures approaching 80 °C since the molecule is not as stable as iodinin (**2**) due to absence of stabilizing intramolecular forces between the 6th positioned phenolic proton and the *N*-oxide placed at the 5th position (Fig. 1). Similar problems were also reported by Zhao and co-workers, attempting to oxidize **14** by the aid of isolated oxidation enzymes from bacteria.³⁶

As a step further, iodinin (**2**) was alkylated using ethyl bromoacetate affording 1-hydroxy-6-(2-ethoxy-2-oxoethoxy)-phenazine 5,10-dioxide (**15**) (Scheme 5). In addition, the dialkylated byproduct **16** was isolated. By similar means, analogues **17** and **18** were afforded from reaction of iodinin with *tert*-butyl bromoacetate to afford the mono- and dialkylated analogues **17** and **18**. *tert*-Butyl ester derivatives **17** and **18** were individually treated with aqueous



Scheme 5. Schematic outline for the synthesis of mono- and dialkylated iodinin esters and carboxylic acids. Reaction conditions: a) ethyl bromoacetate, K₂CO₃, 18-Crown-6, DMF, rt, b) *tert*-Butyl bromoacetate, K₂CO₃, 18-Crown-6, DMF, rt, c) H₃PO₄ (85% aq w/w), DCM, rt.

phosphoric acid which gave the free carboxylic acids **19** and **20** in decent yields. By comparing analogues **15–20** in biological *in vitro* studies we could map the importance of this side chain with an ethyl ester, *tert*-butyl ester and the free carboxylic acid function.

2.2. Evaluation of iodinin analogue effects on intact leukemia cells

2.2.1. Iodinin and its analogues are more potent in 2% than 19% O₂ environment

It is important to know if drug candidates are active in a hypoxic environment, since such an environment is associated with aggressive cancers and poor prognosis.³⁷ Tirapazamine (TPZ, **4**, Fig. 2), which is in phase III clinical trials for chemotherapy against several solid cancers^{38,39} resembles iodinin (**2**) by having a planar aromatic geometry and two *N*-oxides. TPZ (**4**) shows higher activity at low O₂ saturation, thus favouring action in the tumor environment. The bone marrow tends to be hypoxic^{40,41} and although the role of hypoxia in leukemia is not as well understood as for solid cancers, it is associated with poor outcome.⁴² To know if iodinin (**2**) or any of its analogues also were more active at low oxygen saturation, they were tested on MOLM-13 leukemia cells at 2% and near atmospheric (19%) O₂, and the amount of cell death scored (see Table 1 and Fig. 3). Both iodinin (**2**) and several of its analogues, like myxin (**3**), **11** and **14–17** had increased potency (lowered EC₅₀ value) at low O₂ (Table 1). Remarkably, 1-hydroxy-6-methoxyphenazine (**14**) and the corresponding monoxide (**12**) show increased efficacy in 2% O₂ compared to 19% O₂ (Table 1), despite not containing two *N*-oxides like myxin. However, the potency is low compared to myxin (**2**) and similar to what we observe for TPZ (**4**) in hypoxic environment. These compounds might thus be attractive to investigate further as they show very low toxicity at normoxic levels (EC₅₀ > 200 μM for both compounds). The effect of low oxygen saturation became even more apparent for cells pre-incubated at 2% O₂ for two days or longer before being exposed to the compounds (Fig. S-1, suppl. info.). We conclude that not only iodinin (**2**) itself,^{5,20} but also several of its analogues have enhanced activity under hypoxia. They have therefore promise to act more strongly on malignant cells in the hypoxic bone marrow of AML patients than on non-malignant cells in normoxic tissues. To our best knowledge, this is the first time iodinin (**2**) is shown to be hypoxia selective.

Table 1
EC₅₀ values (±SEM) of phenazine-analogues on Molm13 cells.

Compound	EC ₅₀ (μM)	
	19% O ₂	2% O ₂
2 (iodinin)	2.0 ± 0.07	0.79 ± 0.10
3 (myxin)	1.4 ± 0.30	0.77 ± 0.13
4 (TPZ)	95 ± 8*	22 ± 2*
9	72 ± 14*	84 ± 6*
10	100–120*	110–140*
11	4.0 ± 0.48	3.1 ± 0.83
12	>200	22 ± 5
13	5.4 ± 0.68	4.1 ± 0.38
14	>200	39 ± 9
15	0.57 ± 0.06	0.49 ± 0.12
16	2.0 ± 0.47	0.79 ± 0.06
17	2.9 ± 0.34	2.4 ± 0.16
18	4.2 ± 0.20	3.3 ± 0.22
19	54 ± 7	61 ± 4
20	18 ± 3	39 ± 9

The cells were left untreated or treated with various doses of iodinin (**2**) or its analogues for 24 h before cell viability was assessed. The given EC₅₀ values are based on WST-proliferation assay except for those marked with *, which are based on microscopic evaluation of cell death. The data are based on regression analyses of 3 to 4 experiments and are adjusted relative to untreated control cells in each experiment.

2.2.2. Structure-activity relationship of phenazine-analogues and their ability to induce AML cell death

We ensured first that chemically synthesized iodinin (**2**) induced AML cell apoptotic death (Fig. 3A) with similar features as reported previously for iodinin (**2**) isolated from bacteria.^{5,20} The EC₅₀ value of iodinin (**2**) was close to 2 μM (normoxia) whether based on counting of apoptotic cells (Fig. 3A, inset) or spectroscopic evaluation of decline of enzyme activity by the WST-1 method (Fig. 3A). Subsequently, all the synthesized phenazine-analogues were tested for ability to induce death of the human AML cell line MOLM-13, starting with hydroxyl substituents of iodinin (**2**) in the 1st and 6th position and the *N*-oxides in positions 5 and 10 (see Fig. 1 for molecular structure).

When a methoxy group replaced the 6th positioned hydroxyl functionality resulting in the compound myxin (**3**), the cytotoxic potential was found to be unaltered compared to iodinin (**2**) at 2% O₂ (Table 1). However, if both OH-moieties were substituted for methoxy groups (compound **11**), the potency decreased considerably (Table 1). These results are of interest, as myxin (**3**) is already described as an unusually potent antimicrobial agent, possessing broad-spectrum activity against Gram-positive and -negative bacteria while iodinin (**2**) only has weak to moderate antimicrobial effects.⁷ Yet, we observe them to possess approximately equal potencies in inhibition of growth of human AML cells (MOLM-13) at 2% O₂. The far lower activity of tirapazamine (TPZ, **4**), which lacks the oxygen atoms (hydroxy- or methoxy-) adjacent to the *N*-oxide functionalities present in iodinin (**2**) and myxin (**3**), suggests that an electron donating oxygen atom in adjacent position to the *N*-oxide may play an important role for the cytotoxic properties. Moreover, as long as one of the hydroxyl groups is unsubstituted, phenol and methoxy group *O*-substitution seem to result in equal activity. This indicates that one phenolic oxygen of iodinin (**2**) may be functionalized without reducing the cytotoxic activity.

Next, we wanted to investigate if the two *N*-oxides were essential for the cytotoxicity of compound **3** (myxin). We demonstrated that the removal of one *N*-oxide (compound **12**) decreased the cytotoxicity markedly, and that removal of both *N*-oxides produced a compound (**14**) with even less cytotoxicity (Fig 3B and Table 1). These data underpin the importance of di-*N*-oxide functionality for the activity of the PHZ compound class.

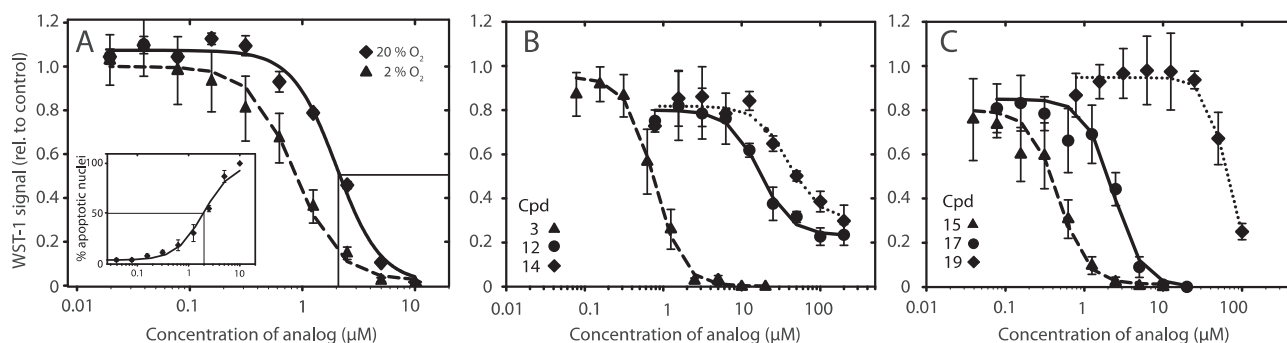


Fig. 3. The cytotoxic effect of iodinin (**2**) and its analogues on the AML cell line MOLM-13. The cells were seeded in 96-well microplates with 20,000 cells/well and immediately exposed to increasing concentrations of iodinin (**2**) or analogues under 2% or 19% oxygen (O₂) for 24 h. Cell proliferation was assessed by the WST-1 assay and by microscopy after Hoechst staining of the cell nuclei. **A:** Cytotoxicity of iodinin at 19% and 2% O₂, measured by the proliferation assay WST-1. The inset shows cytotoxicity at 19% measured by microscopic evaluation of nuclear morphology. **B:** The role of the *N*-oxides in phenazine-induced AML cell death. The MOLM-13 cells were incubated with increasing concentration of 1-hydroxy-6-methoxyphenazine without *N*-oxide (diamonds), with one (circles) or two (triangles) *N*-oxides for 24 h before assessment of viability by the WST-1 assay. **C:** AML cell death inducing activity of iodinin analogues with different substituents on the oxygen in position 6. The data are average of 3–4 experiments and standard error. The lines are from regression analyses as described in the Section 4.

Finally, the phenolic moieties of iodinin (**2**) were mono- and di-functionalized by three different substituents resulting in structures **15–20** (Scheme 5). Substitution of 2-ethoxy-2-oxoethoxy-moiety to the 6th position (compound **15**) enhanced bioactivity substantially while the presence of this substituent in both positions 1 and 6 produced cytotoxicity similar to that of iodinin or myxin (Table 1). A clear trend in these data is therefore that fully oxidized di-alkylated iodinin results in reduced activity compared to mono-alkylated derivatives (see **15** vs **16** and **3** vs. **11** in Table 1).

A puzzling finding was that the addition of a 2-(*tert*-butoxy)2-oxoethoxy (compound **17**) moiety to the 6th positioned oxygen produced a compound with less cytotoxicity than **15**, myxin (**3**) and iodinin (**2**) (see Fig 3C and Table 1). Moreover, if a carboxymethylenoxy moiety was added to the oxygen in the 6th position (compound **19**), the cytotoxicity was about 100-fold less than for the 2-ethoxy-2-oxo-ethoxy substituted analogue **15** (see Fig. 3C and Table 1). A likely explanation is that the carboxyl-group of **19**, predicted to be negatively charged at physiological pH, prevents it from crossing the surface membrane to enter cells. In support of this suggestion, compounds **15** and **17** that carry more lipophilic ester side chains were found to be much more potent. Like myxin (**3**) both of these analogues have greatly enhanced solubility compared to iodinin (**2**) in organic and aqueous media since they lack the intramolecular ion-dipole/hydrogen forces between the 5th positioned *N*-oxide and the phenol hydrogen in the 6th position of iodinin (**2**).

Based on the demonstrated importance of both of the *N*-oxide functionalities (Fig. 3B) and the fact that the 6th positioned hydroxy group can be functionalized without drop in cytotoxic activity, we propose that the ester functionalities of **15**, **16**, and **17** are cleaved off when the compounds have entered the cells and become exposed to the ubiquitous cellular hydrolytic enzymes. If the removal of the moieties happened outside the cells, we would expect also compound **19** to be equally active. The difference in bioactivity between the carboxy-methylenoxy- and the 2-ethoxy-2-oxoethoxy-substituted analogues **19** and **15** is explained if only the latter can cross the membrane to enter the cell where its ester functionality is cleaved off. The superior bioactivity of analogue **15** compared to iodinin (**2**) itself is thus most likely a result of its higher ability to cross biological membranes, although a destabilized *N*-oxide in position 5 due to the lack of intermolecular hydrogen bond from the 6th position might also contribute. Therefore, the 2-ethoxy-2-oxo-ethoxy side chain (compounds **15**, **17** and **19**) chain may be used to influence factors such

as solubility and cell membrane permeability while maintaining or even enhancing the cytotoxic effect by destabilizing and thereby enhancing the reactivity of the *N*-oxide. The enhanced reactivity predicted for compounds **15** and **3** (myxin) may be less important in cells exposed to hypoxia, whose internal ROS level already is high.^{43,44} For targeting cells in hypoxic niches with high internal ROS production, iodinin (**2**) may therefore be more selective than derivatives like myxin (**3**), whose inherent high reactivity may activate them at lower ROS levels as found in normoxic niches.

3. Conclusions

In summary, the chemical part describes for the first time convenient synthetic methods of the literature compounds iodinin (**2**) and myxin (**3**), along with a series of compounds **11–20** derived from them. The key step, revealed to be problematic in previous literature, was the oxidation of 1,6-dihydroxyphenazine (**10**), for which highly efficient oxidation conditions were developed. Since numerous phenazine 5,10-dioxides potentially have exploitable cytotoxic and/or antimicrobial actions, these methods might pave the way for higher synthetic versatility of preparation of novel compounds of this class. Priority was given to produce derivatives that can reveal structure-activity relationships relevant to guide drug development of new anti-leukemic compounds. Synthesized iodinin (**2**) and analogues were evaluated *in vitro* for their ability to induce death of human AML leukemia cells (MOLM-13). We found that one, but not both of the two phenolic functions of iodinin (**2**) can be functionalized synthetically without compromising the cytotoxic activity. In fact, some such derivatives were more potent than iodinin (**2**) itself. In addition, we show that the two *N*-oxides are required for full anti-leukemic effect. The cytotoxic effects provided by iodinin (**2**) and several of its derivatives improved when cells were incubated at hypoxia rather than normoxia, indicating preference for cells in hypoxic niches like the leukemic bone marrow. To our best knowledge, iodinin (**2**) was for the first time shown to be hypoxia selective. Of great importance for the purpose of drug development of this class is the finding that the synthetic ester analogue 1-hydroxy-6-(2-ethoxy-2-oxoethoxy)phenazine (**15**) outperformed both iodinin (**2**) and myxin (**3**) in cytotoxicity assays, most likely as the result of greater cell membrane penetration and more unstable *N*-oxide in its 5th position. Work is in progress to establish a library of screening candidates for broader SAR studies, and to identify potential drug lead candidates for more user-friendly therapeutic regimes against acute myeloid leukemia.

4. Experimental

General information regarding the synthetic work is given within the [Supplementary information](#).

4.1. Synthetic methods

4.1.1. 1,6-Dimethoxyphenazine (**9**)

A dry round-bottom flask with a reflux condenser was charged with 2-bromo-3-methoxyanilin (1.00 g, 4.95 mmol), KHMDS (32 mg, 0.16 mmol, 0.03 eq), BrettPhos Pd G1 Methyl-*t*-Butyl Ether adduct (118 mg, 0.15 mmol, 0.03 eq) and Cs₂CO₃ (3.22 g, 9.88 mmol, 2.0 eq). The system was sealed by a rubber septum before air was removed under reduced pressure and replaced by argon (repeated 3 times). Anhydrous toluene (20 mL) was transferred to the flask and the resulting orange colored suspension gradually warmed up to reflux and left stirring for 24 h. The heating was removed and the crude mixture was cooled to reach rt. The reaction mixture was filtered through a funnel of Celite and undissolved material washed with DCM until no yellow solution came through the funnel. The resulting crude mixture was dry-loaded on silica and purified by flash column chromatography on silica gel (1:7 EtOAc/DCM as eluent) affording 468 mg (79%) of the yellow solid. *R*_f: 0.51 (100% EtOAc). ¹H NMR (400 MHz, CDCl₃) δ 7.99 (dd, *J* = 8.9, 1.1 Hz, 2H), 7.74 (dd, *J* = 8.9, 7.6 Hz, 2H), 7.09 (dd, *J* = 7.6, 1.1 Hz, 2H), 4.17 (s, 6H). ¹³C NMR (101 MHz, CDCl₃) δ 155.1, 143.2, 137.0, 130.3, 122.2, 107.0, 56.6. HRMS (EI): Exact mass calculated for C₁₄H₁₂N₂O₂: 240.0899, found 240.0894 (1.8 ppm). ¹H- and ¹³C NMR data are in accordance with published literature.^{13,45}

4.1.2. 1,6-Dihydroxyphenazine (**10**)

The procedure was performed according to previously described method by Alonso et al.³⁴ Boron tribromide (5.0 g, 20 mmol) was transferred to a dry round-bottom flask containing 1,6-dimethoxyphenazine (**9**) (460 mg, 1.91 mmol) and a magnetic bar under argon atm. The mixture was gradually warmed up 91 °C and refluxed for 5 h. The mixture was cooled on ice bath and carefully quenched by a dropwise addition of ice water and allowed to reach rt. The pH of the solution was adjusted to 7 by 1.0 M NaOH. The goldenrod precipitate was filtered off and washed with cold water. The afforded crude material was dried *in vacuo* yielding 425 mg of 1,6-dihydroxyphenazine (>99%). No further purification was undertaken. *R*_f: 0.42 (100% EtOAc). ¹H NMR (600 MHz, DMSO-*d*₆) δ 10.49 (s, 2H), 7.79–7.70 (m, 4H), 7.19 (dd, *J* = 7.2, 1.4 Hz, 2H). ¹³C NMR (151 MHz, DMSO-*d*₆) δ 153.4, 142.1, 135.7, 131.3, 119.2, 110.6. ¹H- og ¹³C NMR data are in accordance with prior literature.³⁴

4.1.3. 1,6-Dihydroxyphenazine 5,10-dioxide (iodinin; **2**)

A dry round bottomed flask (with a reflux condenser) was loaded with 1,6-dihydroxyphenazine (**10**) (1.23 g, 3.79 mmol) at rt under argon atm. The goldenrod solid was suspended in 100 mL of anhydrous toluene and stirred for 15 min at rt. *m*CPBA (2.0 g, ≤77% purity; Sigma-Aldrich) was added before the mixture was shielded from light and gradually warmed to 80 °C and added 0.80 g *m*CPBA in pulses every hour (i.e. repeated 4 times). After 5 h at 80 °C, 1.0 g of *m*CPBA was added and the reaction mixture stirred for additional 60 min. The reaction mixture was cooled down on ice bath before it was concentrated *in vacuo* to afford dark and slurry crude material. The resulting crude product was dispersed in MeOH/Et₂O (1:1) and filtered on a filter paper in relatively small portions. Each portion was roughly washed by 20 mL NaHCO₃ (saturated aqueous sol.), 20 mL MeOH and 20 mL Et₂O. These portions were collected, combined and washed again by sat-

urated sol. of NaHCO₃ (200 mL), H₂O (50 mL), MeOH (200 mL) and Et₂O (200 mL) or until a homogenous dark-purple color was obtained and clear transparent solvent runs through the filter paper. The remaining product was collected from the filter paper and the product was dried *in vacuo* affording 938 mg (76%) of iodinin (**2**) as a deep-purple solid with a coppery luster. No further purification was necessary. *R*_f: 0.61 (100% DCM). ¹H NMR (600 MHz, DMSO-*d*₆) δ 14.25 (s, 2H), 7.92 (dd, *J* = 9.0, 1.1 Hz, 2H), 7.82 (dd, *J* = 9.0, 7.8 Hz, 2H), 7.19 (dd, *J* = 7.8, 1.1 Hz, 2H). ¹³C NMR (151 MHz, DMSO-*d*₆) δ 152.5, 135.0, 133.4, 126.7, 114.0, 107.4. HRMS (EI): Exact mass calculated for C₁₂H₈N₂O₄: 244.0484, found 244.0487 (−1.2 ppm). ¹H- and ¹³C NMR spectral data are in accordance with prior literature based on isolation of the natural product.²⁰

4.1.4. 1-Hydroxy-6-methoxyphenazine 5,10-dioxide (myxin; **3**)

A dry round-bottom flask was charged with iodinin (**2**) (0.23 g, 0.94 mmol, 1.0 eq), K₂CO₃ (195 mg, 1.41 mmol, 1.5 eq) and 18-Crown-6 (373 mg, 1.41 mmol, 1.5 eq). The solids were dispersed in anhydrous DMF (20 mL) under argon atm and shielded from light. After 30 min of stirring the resulting mixture had switched color from dark violet towards emerald green, a dropwise addition of MeI (0.21 mL, 3.3 mmol, 3.5 eq) was carried out before the mixture was left stirring for an additional period of 24 h at rt. The reaction mixture was concentrated *in vacuo*, diluted by 200 mL of NH₄Cl (10% aqueous sol.) and the aqueous phase extracted by EtOAc (4 × 30 mL). The pooled organic phases were dried with MgSO₄ and filtered. The resulting crude mixture was dry-loaded on silica and further purified by flash column chromatography on silica gel (20–80% EtOAc/Heptan) to afford 175 mg (72%) of myxin (**3**) as a bright cherry-red solid. *R*_f: 0.59 (100% EtOAc). ¹H NMR (600 MHz, CDCl₃) δ 14.59 (broad s, 1H), 8.24 (dd, *J* = 9.1, 1.1 Hz, 1H), 8.03 (dd, *J* = 9.0, 1.1 Hz, 1H), 7.68 (dd, *J* = 9.1, 8.0 Hz, 1H), 7.63 (dd, *J* = 9.1, 7.9 Hz, 1H), 7.12 (dd, *J* = 7.9, 1.1 Hz, 1H), 7.08 (dd, *J* = 8.0, 1.0 Hz, 1H), 4.09 (s, 3H). ¹³C NMR (151 MHz, CDCl₃) δ 153.9, 153.8, 138.8, 136.0, 132.6, 131.8, 130.0, 126.0, 115.0, 110.7, 109.9, 109.0, 57.4. HRMS (EI): Exact mass calculated for C₁₃H₁₀N₂O₄: 258.0641, found 258.0643 (−0.8 ppm). ¹H- and ¹³C NMR data are in accordance with prior literature.^{13,46}

4.1.5. 1,6-Dimethoxyphenazine 5,10-dioxide (**11**)

Isolated as a by-product from the same crude material afforded after the work-up described for the synthesis of myxin (**3**). Flash column chromatography on silica gel (0–3% MeOH/DCM) yielded 30 mg (12%) of the orange solid. *R*_f: 0.06 (100% EtOAc). ¹H NMR (600 MHz, CDCl₃) δ 8.31 (dd, *J* = 9.1, 1.1 Hz, 2H), 7.60 (dd, *J* = 9.1, 7.9 Hz, 2H), 7.08 (dd, *J* = 7.9, 0.7 Hz, 2H), 4.07 (s, 6H). ¹³C NMR (151 MHz, CDCl₃) δ 153.8, 139.7, 130.8, 129.5, 112.3, 110.5, 57.4. HRMS (EI): Exact mass calculated for C₁₄H₁₂N₂O₄: 272.0797, found 272.0795 (0.9 ppm). ¹H- and ¹³C NMR data are in accordance with prior literature.⁴⁵

4.1.6. 1-Hydroxy-6-methoxyphenazine 10-oxide (**12**)

This product was isolated as a by-product from a corresponding crude material afforded after the work-up described for the synthesis of myxin (**3**). Flash column chromatography on silica gel (20–60% EtOAc/Heptane) afforded an orange solid in 18% yield. *R*_f: 0.65 (100% EtOAc). ¹H NMR (400 MHz, CDCl₃) δ 13.63 (s, 1H), 8.14 (dd, *J* = 9.2, 1.1 Hz, 1H), 7.82 (dd, *J* = 8.8, 1.2 Hz, 1H), 7.70 (dd, *J* = 8.8, 7.7 Hz, 1H), 7.67 (dd, *J* = 9.7, 7.7 Hz, 1H), 7.08 (dd, *J* = 7.8, 1.2 Hz, 2H), 4.16 (s, 3H). ¹³C NMR (101 MHz, CDCl₃) δ 155.9, 152.2, 145.3, 139.1, 133.6, 132.5, 131.3, 125.2, 120.2, 113.0, 109.8, 108.3, 56.9. HRMS (EI): Exact mass calculated for C₁₃H₁₀N₂O₃: 242.0691, found 242.0692 (−0.1 ppm). ¹H- and ¹³C NMR data are in accordance with prior literature.^{13,45}

4.1.7. 1,6-Dimethoxyphenazine 5-oxide (**13**)

This product was isolated as a by-product from the same crude material afforded after the work-up described for myxin (**2**). Flash column chromatography on silica gel (0–100% EtOAc/Heptane) afforded 25 mg (10%) of the yellow solid. R_f : 0.18 (100% EtOAc). ^1H NMR (600 MHz, CDCl_3) δ 8.24 (d, J = 9.1 Hz, 1H), 7.92 (d, J = 8.7 Hz, 1H), 7.67–7.56 (m, 2H), 7.07 (d, J = 7.6 Hz, 1H), 7.00 (d, J = 7.8 Hz, 1H), 4.15 (s, 3H), 4.07 (s, 3H). ^{13}C NMR (151 MHz, CDCl_3) δ 155.9, 153.1, 146.7, 138.7, 137.9, 130.5, 129.8, 129.1, 123.3, 111.1, 108.4, 108.3, 57.1, 56.9. HRMS (EI): Exact mass calculated for $\text{C}_{14}\text{H}_{12}\text{N}_2\text{O}_3$: 256.0848, found 256.0851 (–1.2 ppm).

4.1.8. 1-Hydroxy-6-methoxyphenazine (**14**)

MeI (0.11 mL, 1.82 mmol) was added dropwise to a stirring solution of 1,6-dihydroxyphenazine (**10**) (350 mg, 1.65 mmol), K_2CO_3 (228 mg, 1.65 mmol) and 18-Crown-6 (436 mg, 1.65 mmol) in anhydrous DMF (22 mL) at 0 °C. Resulting mixture was left stirring overnight gradually reaching rt concentrated *in vacuo*. The resulting crude redissolved in 40 mL of EtOAc and the organic layer was extracted with 10% NaOH aqueous solution (4 × 30 mL to separate 1-hydroxy-6-methoxy phenazine from the di-methylated byproduct **9**). Basic aqueous fractions were pooled and adjusted to pH 7 by 2 M HCl. The neutral aqueous layer was thereafter extracted by EtOAc (4 × 30 mL). Organic phases pooled, washed with brine (3 × 200 mL), dried over MgSO_4 and concentrated *in vacuo*. The resulting crude was purified by flash column chromatography (10–50% EtOAc/Heptane) affording 89 mg (24%) of yellow solid. R_f : 0.33 (1:1 EtOAc/Heptane). ^1H NMR (400 MHz, CDCl_3) δ 8.19 (s, 1H), 7.94 (dd, J = 8.9, 1.2 Hz, 1H), 7.82 (dd, J = 8.9, 1.2 Hz, 1H), 7.75 (dd, J = 8.9, 7.5 Hz, 2H), 7.29–7.22 (m, 1H), 7.10 (dd, J = 7.5, 1.2 Hz, 1H), 4.19 (s, 3H). ^{13}C NMR (101 MHz, CDCl_3) δ 155.3, 151.5, 142.7, 142.0, 137.7, 134.7, 131.6, 130.7, 121.0, 120.7, 109.5, 107.0, 56.7. ^1H og ^{13}C NMR data are in accordance with literature.¹³

4.1.9. 1-Hydroxy-6-(2-ethoxy-2-oxoethoxy)phenazine 5,10-dioxide (**15**)

A dry round bottom flask was charged with iodinin (180 mg, 0.73 mmol), K_2CO_3 (111 mg, 0.80 mmol) and 18-Crown-6 (212 mg, 0.80 mmol) and a magnetic stir bar. The system was closed by a rubber septum, shielded from light and flushed thoroughly with argon. THF (10 mL) was added to disperse ingredients and the resulting mixture was allowed to rotate for additional 30 min before ethyl bromoacetate (0.07 mL, 0.63 mmol) was added in a drop-wise manner. The reaction was left rotating at rt for 2 h. The reaction mixture was quenched by 50 mL of NH_4Cl (10% aqueous sol.) before the aqueous phase was extracted with EtOAc (4 × 30 mL). Combined organic phases were dried over MgSO_4 , filtered and the resulting solution absorbed onto silica gel. Flash column chromatography on silica (30–100% EtOAc/Heptane) gave 45 mg (17%) of the cherry-red solid. ^1H NMR (600 MHz, CDCl_3) δ 14.52 (s, 1H), 8.34 (dd, J = 9.1, 1.1 Hz, 1H), 8.03 (dd, J = 9.1, 1.1 Hz, 1H), 7.64 (dt, J = 9.0, 7.8 Hz, 2H), 7.13 (dd, J = 7.8, 1.1 Hz, 2H), 4.88 (s, 2H), 4.31 (q, J = 7.1 Hz, 2H), 1.32 (t, J = 7.1 Hz, 3H). ^{13}C NMR (151 MHz, CDCl_3) δ 167.94, 153.89, 151.67, 138.95, 135.97, 132.70, 131.35, 130.64, 126.03, 115.09, 114.58, 113.05, 109.02, 68.38, 61.87, 14.34. HRMS (TOF ES⁺): Exact mass calculated for $\text{C}_{16}\text{H}_{14}\text{N}_2\text{O}_6\text{Na}$ [M+Na]⁺: 353.0749, found 353.0745 (–1.29 ppm).

4.1.10. 1,6-Bis(2-ethoxy-2-oxoethoxy)phenazine 5,10-dioxide (**16**)

This product was isolated as a by-product from the same crude material afforded after the work-up described for compound **15**. Flash column chromatography, first 30–100% EtOAc/heptane to elute out compound **15**, then switching to 1:7 EtOAc/DCM afforded 43 mg (14%) of an orange solid. R_f : 0.23 (3% MeOH/

DCM). ^1H NMR (600 MHz, CDCl_3) δ 8.41 (dd, J = 9.0, 1.2 Hz, 2H), 7.60 (dd, J = 9.1, 7.8 Hz, 2H), 7.16 (dd, J = 7.9, 1.2 Hz, 2H), 4.88 (s, 4H), 4.30 (q, J = 7.1 Hz, 4H), 1.30 (t, J = 7.2 Hz, 6H). ^{13}C NMR (151 MHz, CDCl_3) δ 168.19, 151.66, 139.86, 130.57, 115.66, 114.69, 77.16, 68.68, 61.75, 14.32. HRMS (TOF ES⁺): Exact mass calculated for $\text{C}_{20}\text{H}_{20}\text{N}_2\text{O}_8\text{Na}$ [M+Na]⁺: 439.1117, found 439.1121 (0.82 ppm).

4.1.11. 1-Hydroxy-6-(2-(tert-butoxy)-2-oxoethoxy)phenazine 5,10-dioxide (**17**)

A 50 mL dry round bottom flask was charged with iodinin (158 mg, 0.65 mmol, 1 eq), K_2CO_3 (0.10 g, 0.72 mmol, 1.1 eq) and 18-Crown-6 (0.19 g, 0.72 mmol, 1.1 eq). The flask was sealed by a rubber septum, shielded from light and flushed thoroughly with argon. Anhydrous DMF (5 mL) was added affording an emerald green dispersion which was stirred for 10 min at rt before *tert*-butyl bromoacetate (0.15 mL, 0.98 mmol, 1.5 eq) was added dropwise. The resulting mixture was allowed to stir for 2 h at rt before quenched with NH_4Cl (30 mL of 10% aqueous sol.). The crude mixture was transferred to a separatory funnel and extracted by EtOAc (3 × 30 mL). The organic phase was washed by brine (2 × 200 mL), collected and consequently dry-loaded on silica. Flash column chromatography on silica (10–25% EtOAc/Heptane) afforded 99 mg (43%) of the deep-red solid. R_f : 0.78 (100% EtOAc). ^1H NMR (300 MHz, CDCl_3) δ 14.54 (s, 1H), 8.30 (dd, J = 9.1, 1.1 Hz, 1H), 8.02 (dd, J = 9.0, 1.1 Hz, 1H), 7.69–7.57 (m, 2H), 7.11 (dd, J = 7.9, 1.1 Hz, 1H), 7.06 (dd, J = 7.9, 0.9 Hz, 1H), 4.77 (s, 2H), 1.50 (s, 9H). ^{13}C NMR (151 MHz, CDCl_3) δ 166.8, 153.8, 151.9, 138.9, 136.0, 132.6, 131.4, 130.4, 126.0, 115.0, 113.4, 112.4, 109.1, 83.1, 68.2, 28.2. HRMS (TOF ES⁺): Exact mass calculated for $\text{C}_{18}\text{H}_{18}\text{N}_2\text{O}_6\text{Na}$ [M+Na]⁺: 381.1062, found 381.1058 (–1.20 ppm).

4.1.12. 1,6-Bis(2-(tert-butoxy)-2-oxoethoxy)phenazine 5,10-dioxide (**18**)

A dry roundbottom flask was loaded with iodinin (71 mg, 0.29 mmol, 1 eq), K_2CO_3 (60 mg, 0.44 mmol, 1.5 eq) and 18-crown-6-ether (114 mg, 0.44 mmol, 1.5 eq). The sealed flask was shielded from light and flushed thoroughly with argon before anhydrous THF (4 mL) was added to disperse the ingredients. After 15 min of rotation at rt, *tert*-butyl bromoacetate (0.15 mL, 1.02 mmol) was added dropwise. The resulting mixture was allowed to rotate until no starting material observed by TLC (16 h). The reaction mixture was diluted by 15 mL of DCM and dry loaded directly on silica. Flash column chromatography (10–50% EtOAc in Heptane) afforded 64 mg (47%) of bright-orange-red solid. R_f : 0.43 (100% EtOAc). ^1H NMR (600 MHz, CDCl_3) δ 8.37 (dd, J = 9.0, 1.1 Hz, 2H), 7.56 (dd, J = 9.1, 7.8 Hz, 2H), 7.07 (dd, J = 8.0, 1.2 Hz, 2H), 4.76 (s, 4H), 1.47 (s, 18H). ^{13}C NMR (151 MHz, CDCl_3) δ 167.0, 151.8, 139.8, 130.4, 130.0, 114.4, 114.1, 82.8, 68.4, 28.2. HRMS (TOF ES⁺): Exact mass calculated for $\text{C}_{24}\text{H}_{28}\text{N}_2\text{O}_8\text{Na}$ [M+Na]⁺: 495.1743, found 495.1729 (2.90 ppm).

4.1.13. 1-(Carboxymethoxy)-6-hydroxyphenazine 5,10-dioxide (**19**)

1-(2-(*tert*-Butoxy)-2-oxoethoxy)-6-hydroxyphenazine 5,10-dioxide (**18**) (87 mg, 0.08 mmol) was dissolved in 5 mL DCM. The red solution was cooled on ice bath and 2 mL of H_3PO_4 (85% v/w aqueous sol.) added dropwise. The resulting dispersion was left stirring overnight at reaching rt gradually. The crude mixture was neutralized and pH adjusted to 8 by sat. NaHCO_3 (aqueous sol.). The red aqueous phase was washed with DCM (3 × 20 mL, or until no color was observed within the organic phase). The resulting aqueous phase was collected and pH adjusted to 1 by HCl (37% w/w aqueous sol.). The red precipitate was filtered, washed with H_2O (50 mL), MeOH (20 mL) and Et_2O (40 mL). The filtered product was collected affording 67 mg (92%) of the deep-red solid. No further purification was necessary. ^1H NMR

(400 MHz, DMSO- d_6) δ 14.93 (s, 1H), 13.17 (s, 1H), 8.16 (d, $J = 8.9$ Hz, 1H), 7.89–7.75 (m, 2H), 7.71 (dd, $J = 9.0, 7.8$ Hz, 1H), 7.27 (dd, $J = 8.0, 1.1$ Hz, 1H), 7.12 (dd, $J = 7.9, 1.1$ Hz, 1H), 4.92 (s, 2H). ^{13}C NMR (101 MHz, DMSO- d_6) δ 169.3, 153.1, 151.3, 138.5, 135.5, 132.1, 131.9, 130.0, 125.5, 113.9, 113.3, 111.0, 108.2, 66.9. HRMS (TOF ES $^+$): Exact mass calculated for $\text{C}_{14}\text{H}_9\text{N}_2\text{O}_6$ [M-H] $^-$: 301.0460, found 301.0465 (1.45 ppm).

4.1.14. 1,6-Bis(carboxymethoxy)phenazine 5,10-dioxide (20)

1,6-Bis(2-(*tert*-butoxy)-2-oxoethoxy)phenazine 5,10-dioxide (113 mg, 0.24 mmol) was dissolved in DCM (4 mL) and pipetted dropwise to stirring aqueous solution of H_3PO_4 (3 mL; ≥ 85 wt.% in H_2O). The resulting mixture was stirred for 5 h at room temperature before the mixture was diluted by 50 mL of sat. NaHCO_3 aqueous solution and placed in a separatory funnel. The aqueous phase (orange colored) was washed with 2×20 mL of DCM in order to wash out unreacted starting material. The pH of the aqueous solution was adjusted by dropwise addition of HCl (37% w/v) and the precipitated product filtered and dried affording 76 mg (88%) of the wanted orange solid. No further purification was necessary. ^1H NMR (600 MHz, DMSO- d_6) δ 13.17 (s, 2H), 8.17 (dd, $J = 9.1, 1.1$ Hz, 2H), 7.72 (dd, $J = 9.0, 7.9$ Hz, 2H), 7.30 (dd, $J = 8.0, 1.2$ Hz, 2H), 4.91 (s, 4H). ^{13}C NMR (151 MHz, DMSO- d_6) δ 169.6, 151.4, 139.1, 130.7, 129.3, 114.7, 112.7, 67.6. HRMS (TOF ES $^+$): Exact mass calculated for $\text{C}_{16}\text{H}_{10}\text{N}_2\text{O}_8\text{Na}$ [M-2H+Na] $^+$: 381.0334, found 381.0339 (1.08 ppm).

4.2. Cell Maintenance and experimental conditions

The MOLM-13 cells⁴⁷ were cultured in RPMI medium (R5886) enriched with 10% fetal bovine serum (F7524), 0.2 mM L-glutamine (G7513) and additionally supplemented with 50 IU/mL penicillin and 0.1 mg/mL streptomycin (P0781) (all from Sigma-Aldrich, St. Louis, MO, USA). The cells were grown at a density between 75 and 800×10^3 cl/mL at 37 °C in a humidified atmosphere.

All analogues were dissolved in DMSO at concentrations between 2.5 and 20 mM before testing. For cytotoxic testing, the cells were seeded in 96-well Microplates (#167008, Thermo Scientific™ Nunc™ MicroWell™) with 20,000 cells/well in 100 μL medium. The cells were exposed to various concentrations of iodinin or its analogues for 24 h before assessment of viability by the cell proliferation reagent WST-1, according to the manufacturer's instructions (Roche Diagnostics). The cells were next fixed in 2% buffered formaldehyde (pH 7.4) with the DNA-specific dye Hoechst 33342 (Polysciences Inc.) and scored for percent of dead cells by UV-microscopy based on nuclear morphology.⁴⁸ The highest concentration of analogue corresponded to 1% of DMSO, which alone gave less than 7% cell death as judged by nuclear morphology.

EC_{50} values were determined by analyses of WST-1 signal results as well as microscopic evaluation of cell death by four-parameter regression analyses using the SigmaPlot software (Systat Software Inc. San Jose, CA):

$$Y = \min + \frac{(\max - \min)}{1 + \left(\frac{X}{\text{EC}_{50}}\right)^h}$$

where Y is the response (WST-1 signal or percent apoptosis), \min and \max are minimum and maximum response, X is concentration of analogue, EC_{50} equals the point of inflection, i.e. the point that gives half of maximum response, and h is the Hill's slope of the curve. The two methods gave consistent response curves for each analogue. In cases where the analogues' color interfered with the WST-1 signal, cell counting was used.

Acknowledgements

The work with the project and this paper was supported by NOVO Exploratory Pre Seed Grant no. 4462, the University of Oslo Innovation Fund 2015, the Norwegian Cancer Society, and the Western Norway Regional Health Authorities. The School of Pharmacy, University of Oslo is greatly acknowledged for Ph.D.-ships to EÖV and OAHÅ. We thank Dr. Geir Kildahl-Andersen for valuable assistance on NMR-analysis, and Nina Lied Larsen and Kirsten Brønstad for assistance on cell culture. Our NMR-labs at department of Chemistry, University of Oslo are acknowledged as well for excellent service.

A. Supplementary data

Supplementary data associated with this article can be found, in the online version, at <http://dx.doi.org/10.1016/j.bmc.2017.02.058>.

References

- Laursen JB, Nielsen J. Phenazine natural products: biosynthesis, synthetic analogues, and biological activity. *Chem Rev.* 2004;104:1663–1686.
- Mavrodi DV, Blankenfeldt W, Thomashow LS. Phenazine compounds in fluorescent *Pseudomonas* Spp. biosynthesis and regulation. *Annu Rev Phytopathol.* 2006;44:417–445.
- Guttenberger N, Blankenfeldt W, Breinbauer R. Recent developments in the isolation, biological function, biosynthesis, and synthesis of phenazine natural products. *Bioorg Med Chem.* 2017.
- Turner JM, Messenger AJ. Occurrence, biochemistry and physiology of phenazine pigment production. *Adv Microb Physiol.* 1986;27:211–275.
- Myhren LE, Nygaard G, Gausdal G, et al. Iodinin (1,6-dihydroxyphenazine 5,10-dioxide) from *Streptosporangium* sp. induces apoptosis selectively in myeloid leukemia cell lines and patient cells. *Marine Drugs.* 2013;11:332–349.
- Hollstein U, Van Gemert RJ. Interaction of phenazines with polydeoxyribonucleotides. *Biochemistry.* 1971;10:497–504.
- Weigle M, Maestroni G, Mitrovic M, Leimgruber V. Antimicrobial agents structurally related to myxin. *Antimicrob Agents Chemother.* 1970;10:46–49.
- Behki RM, Lesley SM. Deoxyribonucleic acid degradation and the lethal effect by myxin in *Escherichia coli*. *J Bacteriol.* 1972;109:250–261.
- Kondratyuk TP, Park E-J, Yu R, et al. Novel marine phenazines as potential cancer chemopreventive and anti-inflammatory agents. *Marine Drugs.* 2012;10:451.
- Zhao J, Wu Y, Alfred AT, Wei P, Yang S. Anticancer effects of pyocyanin on HepG2 human hepatoma cells. *Lett Appl Microbiol.* 2014;58:541–548.
- Managò A, Becker KA, Carpinteiro A, et al. *Pseudomonas aeruginosa* pyocyanin induces neutrophil death via mitochondrial reactive oxygen species and mitochondrial acid sphingomyelinase. *Antioxid Redox Signal.* 2015;22:1097–1110.
- Fraser RS, Creanor J. The mechanism of inhibition of ribonucleic acid synthesis by 8-hydroxyquinoline and the antibiotic lomofungin. *Biochem J.* 1975;147:401–410.
- Chowdhury G, Sarkar U, Pullen S, et al. DNA strand cleavage by the phenazine di-N-oxide natural product myxin under both aerobic and anaerobic conditions. *Chem Res Toxicol.* 2012;25:197–206.
- Lavaggi ML, Cabrera M, Pintos C, et al. Novel phenazine 5,10-dioxides release (•)OH in simulated hypoxia and induce reduction of tumour volume in vivo. *ISRN Pharmacol.* 2011;2011:314209.
- Lavaggi ML, Nieves M, Cabrera M, et al. Structural modifications on the phenazine N, N'-dioxide-scaffold looking for new selective hypoxic cytotoxins. *Eur J Med Chem.* 2010;45:5362–5369.
- Davis JG. *Chromobacterium iodinum* (n. sp.), Zentralblatt fuer Bakteriologie, Parasitenkunde, Infektionskrankheiten und Hygiene, Abteilung 2, Naturwissenschaftliche: Allgemeine, Lan. (1939); 100: 273–276.
- Collins MD, Jones D, Keddie RM, Sneath PHA. Reclassification of *Chromobacterium iodinum* (Davis) in a Redefined Genus *Brevibacterium* (Breed) as *Brevibacterium iodinum* nom.rev.; comb.nov. *Microbiology.* 1980;120:1–10.
- McIlwain H. The anti-streptococcal action of iodinin. Naphthaquinones and anthraquinones as its main natural antagonists. *Biochem J.* 1943;37:265–271.
- Oftedal L, Selheim F, Wahlsten M, Sivonen K, Doskeland SO, Herfindal L. Marine benthic cyanobacteria contain apoptosis-inducing activity synergizing with daunorubicin to kill leukemia cells, but not cardiomyocytes. *Marine Drugs.* 2010;8:2659–2672.
- Sletta H, Degnes KF, Herfindal L, et al. Anti-microbial and cytotoxic 1,6-dihydroxyphenazine-5,10-dioxide (iodinin) produced by *Streptosporangium* sp. DSM 45942 isolated from the fjord sediment. *Appl Microbiol Biotechnol.* 2014;98:603–610.
- Hollstein U, Butler PL. Inhibition of ribonucleic acid synthesis by myxin. *Biochemistry.* 1972;11:1345–1350.

22. von Pawel J, von Roemeling R, Gatzemeier U, et al. Tirapazamine plus cisplatin versus cisplatin in advanced non-small-cell lung cancer: a report of the international CATAPULT 1 study group. *J Clin Oncol*. 2000;18:1351–1359.
23. Cimmino A, Evidente A, Mathieu V, et al. Phenazines and cancer. *Nat Product Rep*. 2012;29:487–501.
24. Brown JM, Wilson WR. Exploiting tumour hypoxia in cancer treatment. *Nat Rev Cancer*. 2004;4:437–447.
25. Mimeault M, Batra SK. Frequent gene products and molecular pathways altered in prostate cancer- and metastasis-initiating cells and their progenies and novel promising multitargeted therapies. *Mol Med (Manhasset, NY, United States)*. 2011;17:949–964.
26. Wilson WR, Hay MP. Targeting hypoxia in cancer therapy. *Nat Rev Cancer*. 2011;11:393–410.
27. Deschler B, Lübbert M. Acute myeloid leukemia: epidemiology and etiology. *Cancer*. 2006;107:2099–2107.
28. Lichtman MA. A historical perspective on the development of the cytarabine (7 days) and daunorubicin (3 days) treatment regimen for acute myelogenous leukemia. The 40th anniversary of 7 + 3. *Blood Cells Mol Dis*. 2013;50(2013):119–130.
29. Higby DJ, Wallace Jr HJ, Holland JF. Cis-diamminedichloroplatinum (NSC-119875): a phase I study. *Cancer Chemother Rep*. 1973;57:459–463.
30. Yosioka I, Kidani Y. Studies on phenazines. II Synthesis of iodinin. *Yakugaku Zasshi*. 1952;72:1301–1303.
31. Winkler JD, Twenter BM, Gendrineau T. Synthesis of substituted phenazines via palladium-catalyzed aryl ligation. *Heterocycles*. 2012;84:1345–1353.
32. Wohl A, Aue W. Ueber die Einwirkung von Nitrobenzol auf Anilin bei Gegenwart von Alkali. *Ber Dtsch Chem Ges*. 1901;34:2442–2450.
33. Pachter IJ, Kloetzel MC. The Wohl-Aue reaction. I. Structure of benzo [a] phenazine oxides and syntheses of 1,6-dimethoxyphenazine and 1,6-dichlorophenazine. *J Am Chem Soc*. 1951;73:4958–4961.
34. Mateo Alonso A, Horcajada R, Groombridge HJ, et al. Synthesis of phenazine derivatives for use as precursors to electrochemically generated bases. *Org Biomol Chem*. 2005;3:2832–2841.
35. Leimgruber WM. *Alkylation of iodinin*. (Nutley, NJ), United States: Hoffmann-La Roche Inc.; 1975.
36. Zhao Y, Qian G, Ye Y, et al. Heterocyclic aromatic N-oxidation in the biosynthesis of phenazine antibiotics from *Lysobacter antibioticus*. *Org Lett*. 2016;18:2495–2498.
37. Menon C, Fraker DL. Tumor oxygenation status as a prognostic marker. *Cancer Lett*. 2005;221:225–235.
38. DiSilvestro PA, Ali S, Craighead PS, et al. Phase III randomized trial of weekly cisplatin and irradiation versus cisplatin and tirapazamine and irradiation in stages IB2, IIA, IIB, IIIB, and IVA cervical carcinoma limited to the pelvis: a Gynecologic Oncology Group study. *J Clin Oncol*. 2014;32:458–464.
39. Cohen EEW, Rosine D, Haraf DJ, et al. Phase I trial of tirapazamine, cisplatin, and concurrent accelerated boost reirradiation in patients with recurrent head and neck cancer. *Int J Radiat Oncol Biol Phys*. 2007;67:678–684.
40. Chiarini F, Lonetti A, Evangelisti C, et al. Advances in understanding the acute lymphoblastic leukemia bone marrow microenvironment: from biology to therapeutic targeting. *Biochim Biophys Acta*. 2016;1863:449–463.
41. Spencer JA, Ferraro F, Roussakis E, et al. Direct measurement of local oxygen concentration in the bone marrow of live animals. *Nature (London, UK)*. 2014;508:269–273.
42. Petit C, Gouel F, Dubus I, Heuclin C, Roget K, Vannier JP. Hypoxia promotes chemoresistance in acute lymphoblastic leukemia cell lines by modulating death signaling pathways. *BMC Cancer*. 2016;16:746.
43. Martinez-Sanchez G, Giuliani A. Cellular redox status regulates hypoxia inducible factor-1 activity. Role in tumour development. *J Exp Clin Cancer Res: CR*. 2007;26:39–50.
44. Wu W, Platoshyn O, Firth Amy L, Yuan Jason XJ. Hypoxia divergently regulates production of reactive oxygen species in human pulmonary and coronary artery smooth muscle cells. *Am J Physiol Lung Cell Mol Physiol*. 2007;293:L952–L959.
45. Weigele M, Leimgruber W. The structure of myxin. *Tetrahedron Lett*. 1967;8:715–718.
46. Edwards OE, Gillespie DC. N-dioxides, a new class of amine oxides. *Tetrahedron Lett*. 1966;7:4867–4870.
47. Matsuo Y, Macleod RAF, Uphoff CC, et al. Two acute monocytic leukemia (AML-M5a) cell lines (MOLM-13 and MOLM-14) with interclonal phenotypic heterogeneity showing MLL-AF9 fusion resulting from an occult chromosome insertion, ins(11;9)(q23;p22p23). *Leukemia*. 1997;11:1469–1477.
48. Myhren L, Nilssen IM, Nicolas V, Doeskeland SO, Barratt G, Herfindal L. Efficacy of multi-functional liposomes containing daunorubicin and emetine for treatment of acute myeloid leukemia. *Eur J Pharm Biopharm*. 2014;88:186–193.